INTERNATIONAL JOURNAL FOR NUMERICAL METHODS IN ENGINEERING
Int. J. Numer. Meth. Engng 2002; **54**:1775–1788 (DOI: 10.1002/nme.487)

Frame-indifferent beam finite elements based upon the geometrically exact beam theory

P. Betsch*,† and P. Steinmann

Department of Mechanical Engineering, University of Kaiserslautern, P.O. 3049, 67653 Kaiserslautern, Germany

SUMMARY

This paper describes a new beam finite element formulation based upon the geometrically exact beam theory. In contrast to many previously proposed beam finite element formulations the present discretization approach retains the frame-indifference (or objectivity) of the underlying beam theory. The space interpolation of rotational degrees-of-freedom is circumvented by the introduction of a reparameterization of the weak form corresponding to the equations of motion of the geometrically exact beam theory. Copyright © 2002 John Wiley & Sons, Ltd.

KEY WORDS: non-linear beam elements; finite rotations; constraints

1. INTRODUCTION

The subject of this paper is the design of beam finite elements for the computer simulation of large deformations in space. Starting with the work of Simo [1] the underlying geometrically exact beam theory has been at the heart of many previously published non-linear beam finite element formulations, see e.g. References [2–13]. However, as has been shown recently by Crisfield and Jelenić [11], most of the aforementioned beam finite elements are not invariant under rigid motion. The lack of frame-indifference of those formulations is caused by the discrete strain measures which, as has been shown in Reference [11], do not inherit the objectivity of the underlying continuous beam strains. This discretization deficiency is closely connected with the fact that three-dimensional finite rotations do not commute. The non-vectorial nature of large rotations in conjunction with the space interpolation of vector rotations can thus be identified as the source of the non-objectivity of the discrete beam strains. In fact, finite element discretizations of the geometrically exact beam theory usually rely on the space interpolation of vector rotations. In this connection we refer to Jelenić and Crisfield [10]

*Correspondence to: P. Betsch, Department of Mechanical Engineering, University of Kaiserslautern, P.O. 3049, 67653 Kaiserslautern, Germany
†E-mail: pbetsch@rhrk.uni-kl.de

Contract/grant sponsor: Publishing Arts Research Council; contract/grant number: 98-1846389

Received 5 February 2001
Revised 2 October 2001

for an investigation of alternative interpolation procedures employing (iterative, incremental or total) vector rotations and the related consequences with regard to non-invariance and path-dependence.

In the present work we circumvent the space interpolation of vector rotations. The proposed finite element discretization relies on the isoparametric interpolation of the director vectors which leads to frame-indifferent beam elements. This approach is facilitated by a reparameterization of the commonly applied weak form corresponding to the equations of motion of the geometrically exact beam theory. This reformulation of the weak form is described in detail in Section 2. Corresponding finite element formulations are dealt with in Section 3. An assessment of the numerical performance of the proposed beam finite elements is contained in Section 4. Eventually, conclusions are drawn in Section 5.

2. GEOMETRICALLY EXACT BEAM FORMULATION

2.1. Summary of the underlying beam theory

In this section we give a brief summary of the beam theory relevant for the ensuing computational treatment. We refer to the book of Antman [14] for an exhaustive account of intrinsic and induced rod theories. Starting with the paper of Simo [1], the rod theory considered herein has dominated the recent literature on the computational treatment of beams undergoing large deformations in space, see e.g. References [2–13]. It can be interpreted as a specific version of the special theory of Cosserat rods. The corresponding equations of motion can be written in the classical form (cf. Antman [14], page 263)

$$\begin{aligned} \mathbf{n}_{,s} + \bar{\mathbf{n}} &= A_\varrho \ddot{\boldsymbol{\varphi}} + \ddot{\mathbf{q}} \\ \mathbf{m}_{,s} + \boldsymbol{\varphi}_{,s} \times \mathbf{n} + \bar{\mathbf{m}} &= \mathbf{q} \times \ddot{\boldsymbol{\varphi}} + \dot{\mathbf{h}} \end{aligned} \tag{1}$$

The quantities in (1) will be specified in the following. Throughout this paper the summation convention applies to repeated indices. Furthermore, Greek indices take values 1 and 2, whereas Latin indices range from 1 to 3.

Kinematic assumptions: The motion of the beam in Euclidean 3-space $\mathbb{R}^3$ is restricted by the assumption that the placement of a material point, identified by its position vector $\mathbf{X}(\theta^i) \in \mathbb{R}^3$ in the reference configuration $\mathscr{B}$ at time $t = 0$, can be described by

$$\mathbf{x}(\theta^\alpha, s, t) = \boldsymbol{\varphi}(s, t) + \theta^\alpha \mathbf{d}_\alpha(s, t) \tag{2}$$

Here, θ^i is a triple of convected co-ordinates $(\theta^1, \theta^2, \theta^3 = s) \in \mathbb{R}^3$ with $s \in [0, L] \subset \mathbb{R}$ being the arc-length of the curve $\boldsymbol{\varphi}(s, 0) \in \mathbb{R}^3$. For simplicity of exposition, but without conceptional limitation, $\boldsymbol{\varphi}(s, 0)$ is assumed to coincide with the line of centroids. Then, in (1), $\mathbf{q} = \mathbf{0}$. The orthonormal directors $\mathbf{d}_1(s, t)$, $\mathbf{d}_2(s, t) \in \mathbb{R}^3$, characterize the configuration of the cross-section at s and time t. Furthermore, one defines $\mathbf{d}_3(s, t) = \mathbf{d}_1(s, t) \times \mathbf{d}_2(s, t)$, with $\mathbf{d}_3(s, 0) = \boldsymbol{\varphi}_{,s}(s, 0)$, where the partial derivative $\partial(\bullet)/\partial s$ is abbreviated by $(\bullet)_{,s}$. The director triad $\{\mathbf{d}_k\}$ can be related to an orthonormal basis $\{\mathbf{e}_k\}$ fixed in space by introducing the rotation tensor $\mathbf{R}(s, t) \in \mathrm{SO}(3)$, such that

$$\mathbf{d}_k(s, t) = \mathbf{R}(s, t)\mathbf{e}_k \tag{3}$$

which implies the relation

$$\mathbf{R}(s,t) = \mathbf{d}_k(s,t) \otimes \mathbf{e}_k \tag{4}$$

Accordingly, possible configurations of the beam are defined by

$$\mathbb{Q} = \{(\boldsymbol{\varphi}, \mathbf{R}) : [0, L] \mapsto \mathbb{R}^3 \times \mathrm{SO}(3)\} \tag{5}$$

Concerning the space discretization by means of the finite element method, the main issue concerns the approximation of $\{\mathbf{d}_k\}$, or alternatively $\mathbf{R}$, so as to account for its orthonormality. The orthonormality of $\{\mathbf{d}_k\}$ can also be expressed by means of six independent constraint equations of the form:

$$\mathbf{d}_i \cdot \mathbf{d}_k - \delta_{ik} = 0 \tag{6}$$

where δ_{ik} is the Kronecker delta. The (holonomic) constraints imply that admissible variations of the directors are given by

$$\delta\mathbf{d}_k = \delta\boldsymbol{\theta} \times \mathbf{d}_k \quad \text{with } \delta\boldsymbol{\theta} \in \mathbb{R}^3 \tag{7}$$

or, alternatively,

$$\delta\mathbf{R} = \delta\hat{\boldsymbol{\theta}}\mathbf{R} \quad \text{with } \delta\hat{\boldsymbol{\theta}} \in \mathrm{so}(3) \tag{8}$$

Here $\delta\hat{\boldsymbol{\theta}} \in \mathrm{so}(3)$ is skew-symmetric, i.e. $\delta\hat{\boldsymbol{\theta}} = -(\delta\hat{\boldsymbol{\theta}})^{\mathrm{T}}$, with associated axial vector $\delta\boldsymbol{\theta} \in \mathbb{R}^3$, that is, $\delta\hat{\boldsymbol{\theta}}\mathbf{a} = \delta\boldsymbol{\theta} \times \mathbf{a}$ for all $\mathbf{a} \in \mathbb{R}^3$. In summary, with regard to Equation (2), admissible variations are characterized by $(\delta\boldsymbol{\varphi}, \delta\boldsymbol{\theta}) \in \mathbb{R}^3 \times \mathbb{R}^3$.

Strain measures: The strain-configuration relations pertaining to the beam theory at hand can be written in material form as

$$\begin{aligned} \boldsymbol{\Gamma} &= \mathbf{R}^{\mathrm{T}}\boldsymbol{\varphi}_{,s} - \mathbf{e}_3 = \Gamma_i \mathbf{e}_i \\ \hat{\mathbf{K}} &= \mathbf{R}^{\mathrm{T}}\mathbf{R}_{,s} - (\mathbf{R}^{\mathrm{T}}\mathbf{R}_{,s})|_{t=0} = \hat{K}_{ij}\mathbf{e}_i \otimes \mathbf{e}_j \end{aligned} \tag{9}$$

Since $\hat{\mathbf{K}}$ is skew-symmetric it can be represented alternatively by the associated axial vector $\mathbf{K} \in \mathbb{R}^3$ as (cf. Angeles [15])

$$\mathbf{K} = K_i \mathbf{e}_i \quad \text{with } K_i = \tfrac{1}{2}\varepsilon_{ijk}\hat{K}_{kj} \tag{10}$$

where ε_{ijk} is the alternating symbol. In view of the material strain measures in (9), corresponding spatial strain measures are given by

$$\begin{aligned} \boldsymbol{\gamma} &= \mathbf{R}\boldsymbol{\Gamma} = \Gamma_i \mathbf{d}_i \\ \mathbf{k} &= \mathbf{R}\mathbf{K} = K_i \mathbf{d}_i \end{aligned} \tag{11}$$

An interpretation of the strain variables can be found in Antman [14]. Accordingly, Γ_1 and Γ_2 measure shear, Γ_3 measures dilatation, K_1 and K_2 measure flexure, and K_3 measures torsion.

Constitutive equations: We focus on hyperelastic material models where the stored-energy function W is given in the form $W(\boldsymbol{\Gamma}, \mathbf{K}, s)$. Then the constitutive equations take the form:

$$n_i = \frac{\partial W}{\partial \Gamma_i} \quad \text{and} \quad m_i = \frac{\partial W}{\partial K_i} \tag{12}$$

such that the material resultants read $\mathbf{N}=n_i\mathbf{e}_i$ and $\mathbf{M}=m_i\mathbf{e}_i$. The corresponding spatial resultants are given by the expressions $\mathbf{n}=\mathbf{R}\mathbf{N}=n_i\mathbf{d}_i$ and $\mathbf{m}=\mathbf{R}\mathbf{M}=m_i\mathbf{d}_i$.

Weak form of the equations of motion: A variational statement corresponding to the equations of motion in (1) can be written in the form:

$$G(\boldsymbol{\varphi},\mathbf{R};\delta\boldsymbol{\varphi},\delta\boldsymbol{\theta})=G_{\text{int}}+G_{\text{dyn}}-G_{\text{ext}}=0 \tag{13}$$

Here G_{int} represents the contribution of the internal virtual work given by

$$G_{\text{int}}(\boldsymbol{\varphi},\mathbf{R};\delta\boldsymbol{\varphi},\delta\boldsymbol{\theta})=\int_0^L[\mathbf{N}\cdot\mathbf{R}^{\mathrm{T}}[\delta\boldsymbol{\varphi}_{,s}-\delta\boldsymbol{\theta}\times\boldsymbol{\varphi}_{,s}]+\mathbf{M}\cdot\mathbf{R}^{\mathrm{T}}\delta\boldsymbol{\theta}_{,s}]\,\mathrm{d}s \tag{14}$$

The contribution of the inertial terms is characterized by

$$G_{\text{dyn}}(\boldsymbol{\varphi},\mathbf{R};\delta\boldsymbol{\varphi},\delta\boldsymbol{\theta})=\int_0^L[A_\varrho\ddot{\boldsymbol{\varphi}}\cdot\delta\boldsymbol{\varphi}+[\mathbf{I}_\varrho\dot{\boldsymbol{\omega}}+\boldsymbol{\omega}\times\mathbf{I}_\varrho\boldsymbol{\omega}]\cdot\delta\boldsymbol{\theta}]\,\mathrm{d}s \tag{15}$$

where A_ϱ is the mass density per reference length and $\mathbf{I}_\varrho$ is the time-dependent spatial inertia tensor defined through $\mathbf{I}_\varrho=\mathbf{R}\mathbf{J}_\varrho\mathbf{R}^{\mathrm{T}}$, with

$$\mathbf{J}_\varrho=M_\varrho^{\alpha\alpha}\mathbf{I}-M_\varrho^{\alpha\beta}\mathbf{e}_\alpha\otimes\mathbf{e}_\beta \tag{16}$$

The time-independent components $M_\varrho^{\alpha\beta}=M_\varrho^{\beta\alpha}$ can be interpreted as mass-moments of inertia of the cross-section. The vector $\boldsymbol{\omega}\in\mathbb{R}^3$ in Equation (13) denotes the spatial angular velocity, which, similar to Equations (7) and (8), implies the relations

$$\dot{\mathbf{d}}_k=\boldsymbol{\omega}\times\mathbf{d}_k\quad\text{and}\quad\dot{\mathbf{R}}=\hat{\boldsymbol{\omega}}\mathbf{R} \tag{17}$$

With regard to the equations of motion in (1), $\mathbf{h}=\mathbf{I}_\varrho\boldsymbol{\omega}$ is the relative angular momentum. Furthermore, G_{ext} in Equation (13) accounts for the contribution of external forces $\bar{\mathbf{n}}$ and couples $\bar{\mathbf{m}}$. It assumes the form:

$$G_{\text{ext}}(\boldsymbol{\varphi},\mathbf{R};\delta\boldsymbol{\varphi},\delta\boldsymbol{\theta})=\int_0^L[\bar{\mathbf{n}}\cdot\delta\boldsymbol{\varphi}+\bar{\mathbf{m}}\cdot\delta\boldsymbol{\theta}]\,\mathrm{d}s \tag{18}$$

For simplicity, and without loss of generality, prescribed boundary conditions of the Dirichlet type have been considered exclusively. Accordingly, Equation (13) has to hold for arbitrary $(\delta\boldsymbol{\varphi}(s),\delta\boldsymbol{\theta}(s))\in\mathbb{R}^3\times\mathbb{R}^3$ subject to the conditions $\delta\boldsymbol{\varphi}=\mathbf{0}$ and $\delta\boldsymbol{\theta}=\mathbf{0}$ at the boundaries of the beam, i.e. at the endpoints $s=0$ and L.

Finite element formulations: As mentioned above many finite element formulations for beams undergoing large deformations in space rest on the weak form (13). The particular form of Equation (13) suggests the interpolation of some sort of rotational degrees-of-freedom. However, due to the non-commutativity of finite rotations, the space interpolation of rotational degrees-of-freedom is prone to destroy the objectivity of the strain measures in the discrete model. This has been shown by Crisfield and Jelenić [11]. To overcome this problem, Jelenić and Crisfield [10] propose the interpolation of local rotations with respect to an element-based reference triad, similar to co-rotational finite element formulations, see e.g. Crisfield [16].

In the present work we propose an alternative discretization approach which retains the strain-invariance of the underlying continuous formulation. To this end we recast the weak form (13) in an alternative form.

2.2. Formulation of the weak form in terms of directors

The goal of this section is to parameterize the weak form (13) alternatively by employing the director triad $\{\mathbf{d}_k\}$. This approach will facilitate finite element implementations of the geometrically exact beam theory at hand that do not rely on the interpolation of rotational degrees-of-freedom.

With regard to the constraints in Equation (6), possible configurations of the beam may also be characterized by the constraint set

$$\tilde{\mathbb{Q}} = \{(\boldsymbol{\varphi}, \mathbf{d}_k) : [0, L] \mapsto \mathbb{R}^3 \times \mathbb{R}^{3\times 3} : \mathbf{d}_i \cdot \mathbf{d}_k - \delta_{ik} = 0\} \tag{19}$$

Accordingly, the function space of $\{\mathbf{d}_k\}$ is restricted to a specific manifold defined by the side conditions $\mathbf{d}_i \cdot \mathbf{d}_k - \delta_{ik} = 0$. Using Equation (4), i.e. $\mathbf{R} = \mathbf{d}_k \otimes \mathbf{e}_k$, which implies the relation $\mathbf{R}_{,s} = \mathbf{d}_{k,s} \otimes \mathbf{e}_k$, the material strain measures in Equation $(9)_1$ and (10) can be written in the alternative form:

$$\begin{aligned} \boldsymbol{\Gamma} &= \Gamma_i \mathbf{e}_i \quad \text{with } \Gamma_i = \mathbf{d}_i \cdot \boldsymbol{\varphi}_{,s} - \delta_{i3} \\ \mathbf{K} &= K_i \mathbf{e}_i \quad \text{with } K_i = \tfrac{1}{2}\,\varepsilon_{ijk}[\mathbf{d}_k \cdot \mathbf{d}_{j,s} - (\mathbf{d}_k \cdot \mathbf{d}_{j,s})|_{t=0}] \end{aligned} \tag{20}$$

In addition to that, the following alternative expressions for the linearized strain measures $\delta\boldsymbol{\Gamma}$ and $\delta\mathbf{K}$ can easily be verified:

$$\begin{aligned} \delta\boldsymbol{\Gamma} &= \mathbf{R}^{\mathrm{T}}[\delta\boldsymbol{\varphi}_{,s} - \delta\boldsymbol{\theta} \times \boldsymbol{\varphi}_{,s}] \\ \delta\boldsymbol{\Gamma} &= [\delta\mathbf{d}_i \cdot \boldsymbol{\varphi}_{,s} + \mathbf{d}_i \cdot \delta\boldsymbol{\varphi}_{,s}]\mathbf{e}_i \end{aligned} \tag{21}$$

and

$$\begin{aligned} \delta\mathbf{K} &= \mathbf{R}^{\mathrm{T}}\delta\boldsymbol{\theta}_{,s} \\ \delta\mathbf{K} &= \tfrac{1}{2}\,\varepsilon_{ijk}[\delta\mathbf{d}_k \cdot \mathbf{d}_{j,s} + \mathbf{d}_k \cdot \delta\mathbf{d}_{j,s}]\mathbf{e}_i \end{aligned} \tag{22}$$

Accordingly, an alternative representation of the internal virtual work (14) is given by the expression:

$$\tilde{G}_{\mathrm{int}}(\boldsymbol{\varphi}, \mathbf{d}_k; \delta\boldsymbol{\varphi}, \delta\mathbf{d}_k) = \int_0^L [n_i[\delta\mathbf{d}_i \cdot \boldsymbol{\varphi}_{,s} + \mathbf{d}_i \cdot \delta\boldsymbol{\varphi}_{,s}] + \tfrac{1}{2}\, m_i \varepsilon_{ijk}[\delta\mathbf{d}_k \cdot \mathbf{d}_{j,s} + \mathbf{d}_k \cdot \delta\mathbf{d}_{j,s}]]\,\mathrm{d}s \tag{23}$$

Consider next the virtual work expression (15) corresponding to the inertial terms. A straightforward calculation, based on Equations (16) and (17), yields the relation

$$[\mathbf{I}_\varrho \dot{\boldsymbol{\omega}} + \boldsymbol{\omega} \times \mathbf{I}_\varrho \boldsymbol{\omega}] \cdot \delta\boldsymbol{\theta} = M_\varrho^{\alpha\beta} \ddot{\mathbf{d}}_\alpha \cdot \delta\mathbf{d}_\beta \tag{24}$$

such that an alternative form of G_{dyn} is given by

$$\tilde{G}_{\mathrm{dyn}}(\boldsymbol{\varphi}, \mathbf{d}_\alpha; \delta\boldsymbol{\varphi}, \delta\mathbf{d}_\alpha) = \int_0^L [A_\varrho \ddot{\boldsymbol{\varphi}} \cdot \delta\boldsymbol{\varphi} + M_\varrho^{\alpha\beta} \ddot{\mathbf{d}}_\alpha \cdot \delta\mathbf{d}_\beta]\,\mathrm{d}s \tag{25}$$

If the external loading can be derived from a potential function $\bar{W}(\boldsymbol{\varphi}, \mathbf{d}_k)$, such that

$$\bar{\mathbf{n}} = -\frac{\partial \bar{W}}{\partial \boldsymbol{\varphi}} \quad \text{and} \quad \bar{\mathbf{m}} = -\mathbf{d}_k \times \frac{\partial \bar{W}}{\partial \mathbf{d}_k} \tag{26}$$

the virtual work expression (18) corresponding to the external loading can be rewritten as

$$\tilde{G}_{\text{ext}}(\boldsymbol{\varphi}, \mathbf{d}_k; \delta\boldsymbol{\varphi}, \delta\mathbf{d}_k) = \int_0^L \left[\frac{\partial \bar{W}}{\partial \boldsymbol{\varphi}} \cdot \delta\boldsymbol{\varphi} + \frac{\partial \bar{W}}{\partial \mathbf{d}_k} \cdot \delta\mathbf{d}_k \right] \mathrm{d}s \tag{27}$$

Constrained weak form: In anticipation of our ensuing finite element discretization we next resort to the Lagrange multiplier technique for the enforcement of the side conditions (6). Accordingly, an arbitrary configuration of the beam is specified by $(\boldsymbol{\varphi}, \mathbf{d}_k) \in \mathbb{K}$, with the set $\mathbb{K}$ now given by

$$\mathbb{K} = \{(\boldsymbol{\varphi}, \mathbf{d}_k) : [0, L] \mapsto \mathbb{R}^3 \times \mathbb{R}^{3\times 3}\} \tag{28}$$

In addition to that, we introduce Lagrange multipliers $\lambda_{ij} \in \mathbb{L}$, with

$$\mathbb{L} = \{\lambda_{ij} : [0, L] \mapsto \mathbb{R}^{3\times 3} : \lambda_{ij} = \lambda_{ji}\} \tag{29}$$

The multipliers λ_{ij} are associated with six independent constraint equations $\mathbf{d}_i \cdot \mathbf{d}_j = \delta_{ij}$. The weak form of the equations of motion can now be written as

$$\tilde{G}(\boldsymbol{\varphi}, \mathbf{d}_k, \lambda_{ij}; \delta\boldsymbol{\varphi}, \delta\mathbf{d}_k, \delta\lambda_{ij}) = \tilde{G}_{\text{int}} + \tilde{G}_{\lambda} + \tilde{G}_{\text{dyn}} - \tilde{G}_{\text{ext}} = 0 \tag{30}$$

where $\tilde{G}_{\text{int}}$, $\tilde{G}_{\text{dyn}}$ and $\tilde{G}_{\text{ext}}$ have been specified above and $\tilde{G}_{\lambda}$ is given by

$$\tilde{G}_{\lambda}(\mathbf{d}_k, \lambda_{ij}; \delta\mathbf{d}_k, \delta\lambda_{ij}) = \frac{1}{2} \int_0^L \delta[\lambda_{ij}[\mathbf{d}_i \cdot \mathbf{d}_j - \delta_{ij}]] \, \mathrm{d}s \tag{31}$$

Equation (30) has to be fulfilled for arbitrary $\delta\lambda_{ij} \in \mathbb{L}$ and $(\delta\boldsymbol{\varphi}(s), \delta\mathbf{d}_k(s)) \in \mathbb{R}^3 \times \mathbb{R}^{3\times 3}$, subject to appropriate boundary conditions. In the case of pure Dirichlet boundary conditions $\delta\boldsymbol{\varphi}$ and $\delta\mathbf{d}_k$ have to vanish at the endpoints of the beam.

3. FINITE ELEMENT FORMULATIONS

In this section we present alternative finite element formulations emanating from the weak form (30) pertaining to the geometrically exact beam theory at hand. In contrast to previous finite element formulations based on the geometrically exact beam theory we do not apply any interpolation of rotational degrees-of-freedom.

Let us consider a standard finite element discretization of the domain $[0, L]$ with associated nodal points $A = 1, \ldots, n_{\text{node}}$. Possible configurations of the discrete beam are characterized by nodal quantities $(\boldsymbol{\varphi}^A(t), \mathbf{d}_k^A(t)) \in \mathbb{R}^3 \times \mathbb{R}^{3\times 3}$. The finite element interpolations in space are given by

$$\boldsymbol{\varphi}^h(s,t) = \sum_{A=1}^{n_{\text{node}}} N_A(s)\boldsymbol{\varphi}^A(t) \quad \text{and} \quad \mathbf{d}_k^h(s,t) = \sum_{A=1}^{n_{\text{node}}} N_A(s)\mathbf{d}_k^A(t) \tag{32}$$

where $N_A(s)$ are Lagrange-type nodal shape functions. Similarly, the test functions are approximated by the interpolation formulas

$$\delta\boldsymbol{\varphi}^h(s) = \sum_{A=1}^{n_{\text{node}}} N_A(s)\delta\boldsymbol{\varphi}^A \quad \text{and} \quad \delta\mathbf{d}_k^h(s) = \sum_{A=1}^{n_{\text{node}}} N_A(s)\delta\mathbf{d}_k^A \tag{33}$$

Inserting the above finite element approximations into Equation (23), (25) and (27) yields the discrete versions

$$\begin{aligned} \tilde{G}^h_{\text{int}} &= \tilde{G}_{\text{int}}(\boldsymbol{\varphi}^h, \mathbf{d}^h_k; \delta\boldsymbol{\varphi}^h, \delta\mathbf{d}^h_k) \\ \tilde{G}^h_{\text{dyn}} &= \tilde{G}_{\text{dyn}}(\boldsymbol{\varphi}^h, \mathbf{d}^h_\alpha; \delta\boldsymbol{\varphi}^h, \delta\mathbf{d}^h_\alpha) \\ \tilde{G}^h_{\text{ext}} &= \tilde{G}_{\text{ext}}(\boldsymbol{\varphi}^h, \mathbf{d}^h_k; \delta\boldsymbol{\varphi}^h, \delta\mathbf{d}^h_k) \end{aligned} \tag{34}$$

Before we proceed with the discretization process we show that the discrete strain measures stemming from the interpolation formulas in (32) are invariant under rigid motions.

Objectivity of the discrete strain measures: The discrete counterparts Γ^h_i and K^h_i of the material strains in Equation (20) inherit the objectivity of the underlying geometrically exact beam theory. To see this, consider rigid motions of the discrete beam defined by

$$(\boldsymbol{\varphi}^A)^\sharp = \mathbf{c} + \mathbf{Q}\boldsymbol{\varphi}^A \quad \text{and} \quad (\mathbf{d}^A_k)^\sharp = \mathbf{Q}\mathbf{d}^A_k \tag{35}$$

with $\mathbf{c}(t) \in \mathbb{R}^3$ and $\mathbf{Q}(t) \in \mathrm{SO}(3)$. With regard to Equation (20) and (32), one gets

$$\begin{aligned} (\Gamma^h_i)^\sharp &= (\mathbf{d}^h_i)^\sharp \cdot (\boldsymbol{\varphi}^h_{,s})^\sharp - \delta_{i3} \\ (\Gamma^h_i)^\sharp &= \sum_{A,B=1}^{n_{\text{node}}} N_A N_{B,s} \, (\mathbf{d}^A_i)^\sharp \cdot (\boldsymbol{\varphi}^B)^\sharp - \delta_{i3} \\ (\Gamma^h_i)^\sharp &= \sum_{A,B=1}^{n_{\text{node}}} N_A N_{B,s} \, [\mathbf{Q}\mathbf{d}^A_i] \cdot [\mathbf{c} + \mathbf{Q}\boldsymbol{\varphi}^B] - \delta_{i3} \end{aligned} \tag{36}$$

Due to the completeness condition $\sum_{B=1}^{n_{\text{node}}} N_B(s) = 1$, one has $\sum_{B=1}^{n_{\text{node}}} N_{B,s}\,\mathbf{c} = \mathbf{0}$. Further, $[\mathbf{Q}\mathbf{d}^A_i] \cdot [\mathbf{Q}\boldsymbol{\varphi}^B] = \mathbf{d}^A_i \cdot \mathbf{Q}^{\mathrm{T}}\mathbf{Q}\boldsymbol{\varphi}^B = \mathbf{d}^A_i \cdot \boldsymbol{\varphi}^B$, such that

$$(\Gamma^h_i)^\sharp = \sum_{A,B=1}^{n_{\text{node}}} N_A N_{B,s} \, \mathbf{d}^A_i \cdot \boldsymbol{\varphi}^B - \delta_{i3} \tag{37}$$

which implies that

$$(\Gamma^h_i)^\sharp = \Gamma^h_i \quad \forall s \in [0, L] \tag{38}$$

Similarly, one gets $(K^h_i)^\sharp = K^h_i$ for all $s \in [0, L]$. Accordingly, the discrete strain measures corresponding to the interpolation formulas in Equation (32) are invariant under rigid motions. In contrast to that, most beam elements based on the interpolation of rotational degrees-of-freedom fail to be frame-indifferent, see Crisfield and Jelenić [11].

Treatment of the director constraints: In order to complete the space discretization of the weak form (30), it remains to specify the treatment of the test and trial functions associated with the Lagrange multipliers for the enforcement of the orthonormality of $\{\mathbf{d}^h_k\}$. To this end we choose

$$\lambda^h_{ij}(s,t) = \sum_{A=1}^{n_{\text{node}}} M_A(s)\lambda^A_{ij}(t) \quad \text{and} \quad \delta\lambda^h_{ij}(s) = \sum_{A=1}^{n_{\text{node}}} M_A(s)\delta\lambda^A_{ij} \tag{39}$$

where the basis functions $M_A(s)$ coincide with Dirac deltas associated with the nodal points s_A, $A = 1, \ldots, n_{\text{node}}$, of the finite element discretization. Accordingly, we set

$$M_A(s) = \delta(s - s_A) \tag{40}$$

such that the corresponding discrete version of Equation (31) assumes the particular form:

$$\tilde{G}^h_\lambda = \tilde{G}_\lambda(\mathbf{d}^h_k, \lambda^h_{ij}; \delta\mathbf{d}^h_k, \delta\lambda^h_{ij}) = \frac{1}{2}\sum_{A=1}^{n_{\text{node}}} \delta\lambda^A_{ij}[\mathbf{d}^A_i \cdot \mathbf{d}^A_j - \delta_{ij}] + \sum_{A=1}^{n_{\text{node}}} \lambda^A_{ij}\delta\mathbf{d}^A_i \cdot \mathbf{d}^A_j \tag{41}$$

Our approach can be interpreted as collocation method where the finite element nodes serve as collocation points for the enforcement of the director constraints. Accordingly, orthonormality of the discrete director field is confined to the nodal points.

3.1. Constrained finite element formulation

From here onwards, we restrict ourselves to the static case. Issues pertaining to the time discretization for the dynamic case are discussed in a forthcoming work. For the static case, substitution of the above finite element expressions into the weak form of equilibrium (30) leads to the equations

$$\begin{aligned}[\tilde{G}^h_{\text{int}} - \tilde{G}^h_{\text{ext}}](\boldsymbol{\varphi}^A, \mathbf{d}^A_k; \delta\boldsymbol{\varphi}^A, \delta\mathbf{d}^A_k) + \sum_{A=1}^{n_{\text{node}}} \lambda^A_{ij}\delta\mathbf{d}^A_i \cdot \mathbf{d}^A_j &= 0 \\ \sum_{A=1}^{n_{\text{node}}} \delta\lambda^A_{ij}[\mathbf{d}^A_i \cdot \mathbf{d}^A_j - \delta_{ij}] &= 0\end{aligned} \tag{42}$$

which have to hold for arbitrary $(\delta\boldsymbol{\varphi}^A, \delta\mathbf{d}^A_k, \delta\lambda^A_{ij})$, $A = 1, \ldots, n_{\text{node}}$, which, of course, have to conform with the boundary conditions. The resulting system of non-linear equations can be solved for the nodal quantities $(\boldsymbol{\varphi}^A, \mathbf{d}^A_k, \lambda^A_{ij})$ by applying any standard iterative solution procedure, e.g. the Newton–Raphson method.

3.2. Unconstrained finite element formulation

The number of nodal unknowns can be reduced significantly by employing a nodal reduction procedure that does not change the above finite element approximation of possible beam configurations. The nodal reduction procedure relies on the introduction of nodal rotational degrees-of-freedom. In view of (3) each nodal director frame $\{\mathbf{d}^A_i\}$, $A = 1, \ldots, n_{\text{node}}$, can be specified by a rotation tensor $\mathbf{R}^A \in \text{SO}(3)$, so that

$$\mathbf{d}^A_i = \mathbf{R}^A\mathbf{e}_i \tag{43}$$

Then, with regard to Equation (7), admissible variations of the nodal directors take the form:

$$\delta\mathbf{d}^A_i = \delta\boldsymbol{\theta}^A \times \mathbf{d}^A_i \quad \text{with } \delta\boldsymbol{\theta}^A \in \mathbb{R}^3 \tag{44}$$

Within the iterative solution procedure a convenient update of the nodal director frame $\{\mathbf{d}^{A^{(k+1)}}_i\}$ can be accomplished via the multiplicative update formula

$$\mathbf{R}^{A^{(k+1)}} = \exp(\Delta\hat{\boldsymbol{\theta}}^A)\mathbf{R}^{A^{(k)}} \tag{45}$$

where (k) is the iteration index, $\Delta\boldsymbol{\theta}^A \in \mathbb{R}^3$ contains three nodal iterative rotational degrees-of-freedom and $\exp(\Delta\hat{\boldsymbol{\theta}}^A) \in \text{SO}(3)$ denotes the closed-form expression of the exponential map often referred to as the Rodrigues formula, see e.g. Reference [16]. A survey of alternative rotational update concepts can be found in Reference [17].

Application of the proposed nodal reduction procedure to the constrained finite element formulation (42) yields the unconstrained formulation:

$$[\hat{G}^h_{\text{int}} - \hat{G}^h_{\text{ext}}](\boldsymbol{\varphi}^A, \mathbf{d}^A_k; \delta\boldsymbol{\varphi}^A, \delta\boldsymbol{\theta}^A) = 0 \tag{46}$$

which has to hold for arbitrary $(\delta\boldsymbol{\varphi}^A, \delta\boldsymbol{\theta}^A)$, again subject to appropriate boundary conditions. Here $\hat{G}^h_{\text{int}}$ follows from $(34)_1$ by inserting (44) which gives

$$\begin{aligned}\bar{G}_{\text{int}}(\boldsymbol{\varphi}^A, \mathbf{d}^A_k; \delta\boldsymbol{\varphi}^A, \delta\boldsymbol{\theta}^A) = \sum_{A=1}^{n_{\text{node}}} \left[\delta\boldsymbol{\theta}^A \cdot \left[\mathbf{d}^A_i \times \int_0^L N_A n_i \boldsymbol{\varphi}^h_{,s} \, \mathrm{d}s \right] + \delta\boldsymbol{\varphi}^A \cdot \int_0^L N_{A,s} \, n_i \mathbf{d}^h_i \, \mathrm{d}s \right] \\ + \frac{1}{2} \sum_{A=1}^{n_{\text{node}}} \delta\boldsymbol{\theta}^A \cdot \left[\varepsilon_{ijk} \mathbf{d}^A_k \times \int_0^L m_i [N_A \mathbf{d}^h_{j,s} - N_{A,s} \, \mathbf{d}^h_j] \, \mathrm{d}s \right]\end{aligned} \tag{47}$$

Similarly, $\hat{G}^h_{\text{ext}}$ can be obtained from Equation $(34)_3$. Owing to the arbitrariness of $(\delta\boldsymbol{\varphi}^A, \delta\boldsymbol{\theta}^A)$, (46) represents a system of non-linear algebraic equations. They can be customarily solved for the nodal quantities $(\boldsymbol{\varphi}^A, \Delta\boldsymbol{\theta}^A)$ by applying standard iterative solution procedures.

4. REPRESENTATIVE NUMERICAL INVESTIGATIONS

In this section we investigate the numerical performance of the newly developed beam finite elements. Our numerical experiments confirmed that the constrained formulation in Section 3.1 and the unconstrained formulation in Section 3.2 yield identical numerical results. Therefore, we only report on the results of the unconstrained formulation which we call in the following the '$\mathbf{d}_i$ formulation'.

For comparison, we also implemented the beam element due to Simo and Vu-Quoc [2] which is based on the interpolation of iterative rotations. We call this formulation in the following the '$\Delta\boldsymbol{\theta}$ formulation'.

In the numerical examples hyperelastic material behaviour is assumed to be governed by the stored-energy function

$$W(\boldsymbol{\Gamma}, \mathbf{K}) = \tfrac{1}{2} \boldsymbol{\Gamma} \cdot \mathbf{D}_1 \boldsymbol{\Gamma} + \tfrac{1}{2} \mathbf{K} \cdot \mathbf{D}_2 \mathbf{K} \tag{48}$$

with

$$\mathbf{D}_1 = \text{Diag}[GA_1, GA_2, EA] \quad \text{and} \quad \mathbf{D}_2 = \text{Diag}[EI_1, EI_2, GJ] \tag{49}$$

Reduced quadrature formulas are applied, that is, one Gauss point for the linear elements and two Gauss points for the quadratic elements.

4.1. Planar equilibrium problems

Our numerical investigations focus first on planar equilibrium problems. In the planar case finite rotations commute so that the interpolation of rotational degrees-of-freedom in general retains the objectivity of the underlying beam theory. The main purpose of this section is to demonstrate that our advocated $\mathbf{d}_i$ formulation is competitive with well-established formulations based on the interpolation of rotational degrees-of-freedom.

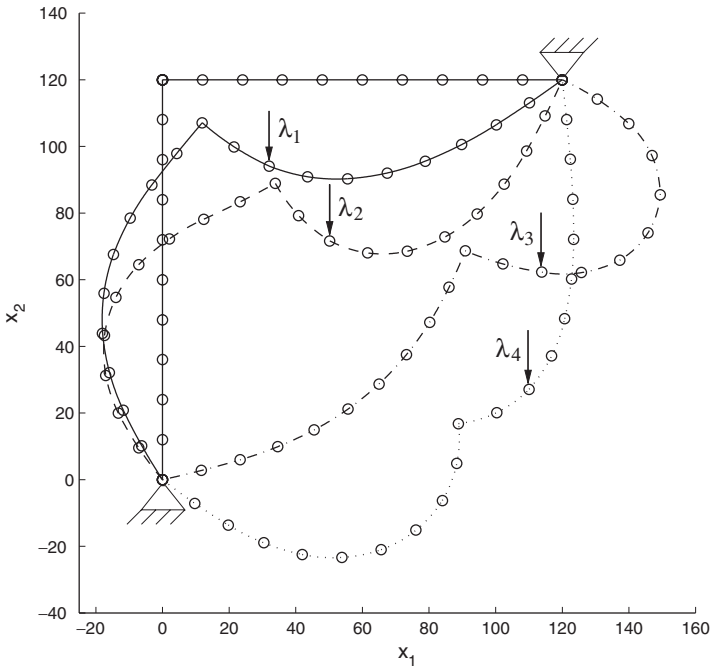

Figure 1. Buckling of a hinged right-angle frame: initial mesh and deformed configurations corresponding to load-level parameters $\lambda_1 = 15$, $\lambda_2 = 18.495$, $\lambda_3 = -9.233$ and $\lambda_4 = 21.014$.

A comparatively demanding planar example consists of the buckling of a hinged right-angle frame, see Figure 1. The data for this example have been taken from Reference [2]. Accordingly, $GA = 16.62 \times 10^6$, $EA = 43.20 \times 10^6$, $EI = 14.40 \times 10^6$ and $GJ = 11.08 \times 10^6$. Ten quadratic elements are used to discretize the problem. A dead load $\mathbf{F} = -\lambda \times 10^3 \mathbf{e}_2$ is applied to the node with position vector $\boldsymbol{\varphi} = 24\mathbf{e}_1 + 120\mathbf{e}_2$ in the undeformed configuration (see Figure 1). Both the $\mathbf{d}_i$ formulation and the $\Delta\boldsymbol{\theta}$ formulation lead to practically indistinguishable results as can be seen from Figure 2 which shows the load-displacement curves for the node under the load. Furthermore, Figure 1 depicts a number of deformed configurations corresponding to the load-level parameters $\lambda_1 = 15$, $\lambda_2 = 18.495$, $\lambda_3 = -9.233$ and $\lambda_4 = 21.014$. The results have been obtained by employing a standard arc-length method (see e.g. Crisfield [18]).

4.2. *Spatial equilibrium problems*

As a representative example for spatial equilibrium problems we consider next the well-known cantilever bend depicted in Figure 3. The stiffness properties are $GA_1 = GA_2 = 5 \times 10^6$, $EA = 10^7$ and $EI_1 = EI_2 = GJ = 10^7/12$. The bend is clamped at one end and a force $\mathbf{F} = F\mathbf{e}_2$ with constant magnitude $F = 600$ acts on the other end.

We investigate first the convergence properties of the beam formulations at hand. To this end, Figure 4 shows the results for the displacement component u_2 under the load for various uniform meshes. Accordingly, for the coarse mesh consisting of 8 linear elements the relative difference between the $\mathbf{d}_i$ and $\Delta\boldsymbol{\theta}$ formulation is only about two per cent. Similarly, for the

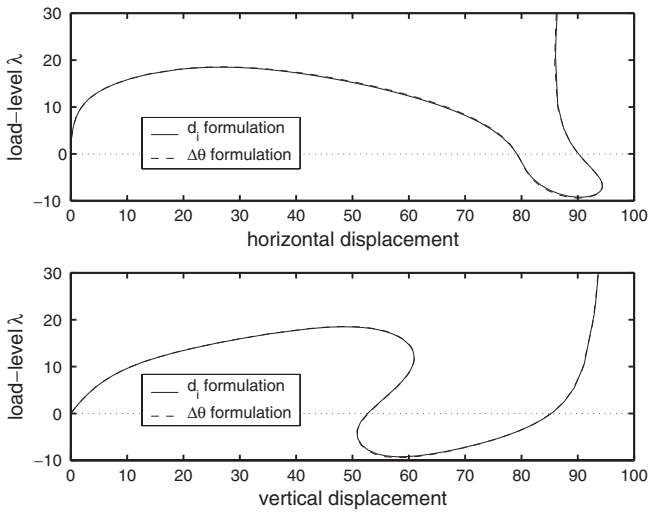

Figure 2. Buckling of a hinged right-angle frame: load-displacement curves under the load.

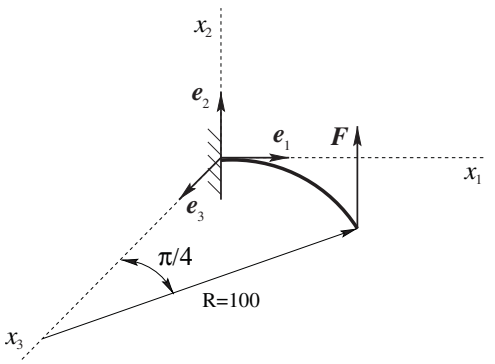

Figure 3. 3D cantilever bend: problem description.

coarse mesh consisting of four quadratic elements the relative difference between the $\mathbf{d}_i$ and $\Delta\boldsymbol{\theta}$ formulation is less than 0.2 per cent.

4.2.1. Numerical objectivity test. We give next a numerical verification of the objectivity property of the $\mathbf{d}_i$ formulation. To this end, we consider again the cantilever bend in Figure 3. Instead of the constant force $\mathbf{F} = F\mathbf{e}_2$ in the previous example, we now apply a loading cycle as depicted in Table I. Accordingly, starting from the force-free initial (natural) configuration (initial load level $[0,0,0]$), the components F_i of the tip force $\mathbf{F} = F_i\mathbf{e}_i$ are prescribed by a sequence of load levels as indicated in Table I. Each load level is obtained from the previous one by applying load increments of magnitude $|\Delta F_i| = 25$. After the loading cycle has been finished (final load level $[0,0,0]$) the final beam configuration has to coincide again with the initial configuration. Indeed, this is generally the case for the $\mathbf{d}_i$ formulation,

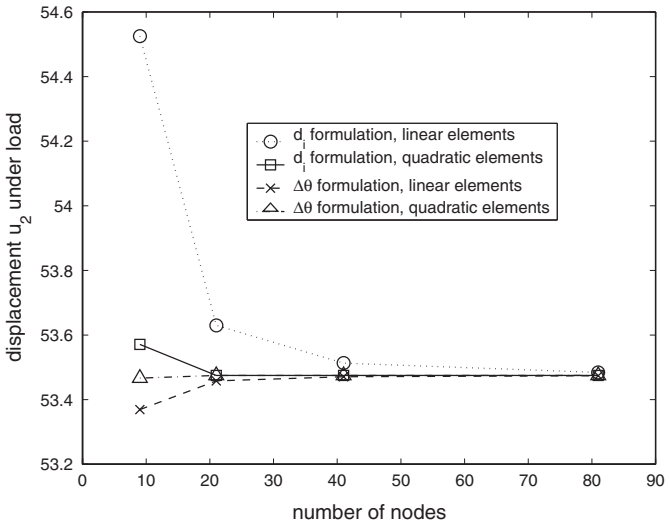

Figure 4. 3D cantilever bend: displacement u_2 under load versus number of nodes.

Table I. Numerical objectivity test: tip displacement u_2 of the cantilever bend corresponding to specific load levels of the loading cycle.

Load level	$\Delta\boldsymbol{\theta}$ formulation			$\mathbf{d}_i$ formulation		
$[F_1, F_2, F_3]$	8 el.	16 el.	32 el.	8 el.	16 el.	32 el.
[0,0,0]	0	0	0	0	0	0
$[-600, 0, 0]$	0	0	0	0	0	0
$[-600, 600, 0]$	59.1177	59.6527	59.7884	61.3302	60.1177	59.9022
$[-600, 600, 600]$	38.1955	38.5701	38.6655	40.0323	38.9342	38.7539
$[0, 600, 600]$	37.1012	37.4262	37.5087	38.3769	37.7264	37.5829
$[0, 0, 600]$	−0.3022	−0.0769	0.0190	5.5×10^{-15}	-5.9×10^{-15}	9.5×10^{-15}
$[0, 0, 0]$	−0.5820	−0.1487	0.0374	5.3×10^{-15}	-3.0×10^{-15}	8.2×10^{-15}

since, with regard to Table I, the final displacement component u_2 equals zero (up to numerical round-off). Analogous observations hold for the two remaining displacement components of the tip displacement. As convergence criteria for the Newton–Raphson equilibrium iterations we prescribed $|\mathbf{R}| < 10^{-7}$, where $|\mathbf{R}|$ denotes the Euclidean norm of the residual vector. The convergence rate observed during the last load step (leading to the final displacement $u_2 = 5.3 \times 10^{-15}$ for the case of 8 elements in Table I) is shown in Table II.

On the other hand, due to the non-invariance and path-dependence of the $\Delta\boldsymbol{\theta}$ formulation, the final configuration does not coincide with the initial configuration anymore. It can be observed from Table I that this pathological behaviour diminishes if the number of nodes is increased. This observation is in agreement with the investigations of the non-objectivity of various beam elements in Reference [10]. In the numerical calculations the convergence criteria was again $|\mathbf{R}| < 10^{-7}$. The convergence rate observed during the last load step (leading

Table II. $\mathbf{d}_i$ formulation.

Iteration number	Euclidean norm of residual
1	2.50×10^{1}
2	3.08×10^{4}
3	5.24×10^{1}
4	5.26×10^{1}
5	3.79×10^{-4}
6	7.81×10^{-8}

Table III. $\Delta\boldsymbol{\theta}$ formulation.

Iteration number	Euclidean norm of residual
1	2.50×10^{1}
2	2.96×10^{4}
3	2.14×10^{1}
4	5.70×10^{1}
5	3.99×10^{-6}
6	1.08×10^{-8}

to the final displacement $u_2 = -0.5820$ for the case of 8 elements in Table I) is shown in Table III.

5. CONCLUSIONS

Two characteristic properties of the geometrically exact beam theory considered herein are (i) the objectivity of the strain measures and (ii) the orthonormality of the director frame. Most previously developed beam finite elements conserve property (ii) throughout the element but sacrifice property (i). The lack of frame-indifference is especially pronounced in the case of course meshes and if large rigid motions appear. On the other hand, our newly proposed discretization approach preserves the fundamental property (i) while property (ii) is confined to the nodal points. Our numerical examples indicate that the relaxation of the orthonormality property does not deteriorate the numerical performance of the newly developed beam elements.

In comparison with previously developed beam finite elements the main difference of the present discretization approach lies in the reparameterization of the variational beam equations in conjunction with the isoparametric interpolation of the director field. There exist several alternative methods for the enforcement of the orthonormality constraint on the *nodal* directors. One may either deal directly with the constrained formulation (as in Section 3.1) or reduce the number of unknowns by employing either total, incremental or iterative (as in Section 3.2) *nodal* rotational degrees-of-freedom.

Our numerical investigations presented herein have been confined to the static case. The dynamic case will be dealt with in a forthcoming work. Due to the specific form of the reparameterized variational beam equations and the fact that the use of rotational degrees-of-freedom is restricted to the nodes, the present beam formulation fits well into the framework for the time discretization proposed in References [19–21].

We finally remark that the beam theory used herein has to be distinguished from continuum-based degenerate beam formulations which usually employ a covariant representation of the Green–Lagrangean strains. For recent developments in this context we refer to Gruttmann *et al*. [22, 23] and references therein.

REFERENCES

1. Simo JC. A finite strain beam formulation. The three-dimensional dynamic problem. Part I. *Computer Methods in Applied Mechanics and Engineering* 1985; **49**:55–70.
2. Simo JC, Vu-Quoc L. A three-dimensional finite-strain rod model. Part II: Computational aspects. *Computer Methods in Applied Mechanics and Engineering* 1986; **58**:79–116.
3. Vu-Quoc L, Simo JC. Dynamics of earth-orbiting flexible satellites with multibody components. *Journal of Guidance, Control and Dynamics* 1987; **10**(6):549–558.
4. Simo JC, Vu-Quoc L. On the dynamics in space of rods undergoing large motions—A geometrically exact approach. *Computer Methods in Applied Mechanics and Engineering* 1988; **66**:125–161.
5. Cardona A, Géradin M. A beam finite element non-linear theory with finite rotations. *International Journal for Numerical Methods in Engineering* 1988; **26**:2403–2438.
6. Simo JC, Tarnow N, Doblare M. Non-linear dynamics of three-dimensional rods: Exact energy and momentum conserving algorithms. *International Journal for Numerical Methods in Engineering* 1995; **38**:1431–1473.
7. Jelenić G, Crisfield MA. Non-linear 'master-slave' relationships for joints in 3D beams with large rotations. *Computer Methods in Applied Mechanics and Engineering* 1996; **135**:211–228.
8. Jelenić G, Crisfield MA. Interpolation of rotational variables in non-linear dynamics of 3D beams. *International Journal for Numerical Methods in Engineering* 1998; **43**:1193–1222.
9. Ibrahimbegović A, Al Mikdad M. Finite rotations in dynamics of beams and implicit time-stepping schemes. *International Journal for Numerical Methods in Engineering* 1998; **41**:781–814.
10. Jelenić G, Crisfield MA. Geometrically exact 3D beam theory: implementation of a strain-invariant finite element for statics and dynamics. *Computer Methods in Applied Mechanics and Engineering* 1999; **171**:141–171.
11. Crisfield MA, Jelenić G. Objectivity of strain measures in the geometrically exact three-dimensional beam theory and its finite-element implementation. *Proceedings of the Royal Society, London Series A* 1999; **455**: 1125–1147.
12. Ibrahimbegović A, Mamouri S. On rigid components and joint constraints in non-linear dynamics of flexible multibody systems employing 3d geometrically exact beam model. *Computer Methods in Applied Mechanics and Engineering* 2000; **188**:805–831.
13. Jelenić G, Crisfield MA. Dynamic analysis of 3D beams with joints in presence of large rotations. *Computer Methods in Applied Mechanics and Engineering* 2001; **190**:4195–4230.
14. Antman SS. *Nonlinear problems of elasticity*. Springer: Berlin, 1995.
15. Angeles J. *Rational Kinematics*. Springer: Berlin, 1988.
16. Crisfield MA. *Non-linear Finite Element Analysis of Solids and Structures. Volume 2: Advanced Topics*. Wiley: New York, 1997.
17. Betsch P, Menzel A, Stein E. On the parameterization of finite rotations in computational mechanics. A classification of concepts with application to smooth shells. *Computer Methods in Applied Mechanics and Engineering* 1998; **155**:273–305.
18. Crisfield MA. *Non-linear Finite Element Analysis of Solids and Structures. Volume 1: Essentials*. Wiley: New York, 1991.
19. Betsch P, Steinmann P. Conservation properties of a time FE method. Part I: Time-stepping schemes for N-body problems. *International Journal for Numerical Methods in Engineering* 2000; **49**:599–638.
20. Betsch P, Steinmann P. Conservation properties of a time FE method. Part II: Time-stepping schemes for non-linear elastodynamics. *International Journal for Numerical Methods in Engineering* 2001; **50**:1931–1955.
21. Betsch P, Steinmann P. Conservation properties of a time FE method. Part III: Mechanical systems with holonomic constraints. *International Journal for Numerical Methods in Engineering* 2002; **53**:2271–2304.
22. Gruttmann F, Sauer R, Wagner W. A geometrical non-linear eccentric 3D-beam element with arbitrary cross-sections. *Computer Methods in Applied Mechanics and Engineering* 1998; **160**:383–400.
23. Gruttmann F, Sauer R, Wagner W. Theory and numerics of three-dimensional beams with elastoplastic material behaviour. *International Journal for Numerical Methods in Engineering* 2000; **48**:1675–1702.

